Rapid and selective screening of organic peroxide explosives using acid-hydrolysis induced chemiluminescence

Mahbub, Parvez, Hasan, Chowdhury, Rudd, David, Voelcker, Nicolas Hans, Orbell, John, Cole, Ivan and Macka, Mirek (2023) Rapid and selective screening of organic peroxide explosives using acid-hydrolysis induced chemiluminescence. Analytica Chimica Acta, 1255. ISSN 0003-2670

Rapid and selective screening of organic peroxide explosives using acid-hydrolysis induced chemiluminescence

Parvez Mahbub[a]*, Chowdhury Kamrul Hasan[a], David Rudd[b,c], Nicolas Hans Voelcker[b,c,d], John Orbell[a], Ivan Cole[e], Mirek Macka[f,g,h]

[a]Institute for Sustainable Industries and Liveable Cities (ISILC), Victoria University, Werribee, Victoria 3030, Australia

[b]Melbourne Centre for Nanofabrication, Victorian Node of the Australian Fabrication Facility, Clayton, Victoria 3168, Australia

[c]Drug Delivery, Disposition and Dynamics, Monash Institute of Pharmaceutical Sciences, Faculty of Pharmacy and Pharmaceutical Sciences, Monash University, Melbourne, Australia

[d]Commonwealth Scientific and Industrial Research Organization (CSIRO), Clayton, Victoria, 3168, Australia

[e]Research & Innovation Portfolio, RMIT University, Melbourne, Australia

[f]Australian Centre for Research on Separation Science (ACROSS), University of Tasmania, Hobart, Australia

[g]Central European Institute of Technology, Brno University of Technology, Purkynova 123, CZ-612 00, Brno, Czech Republic

[h]Department of Chemistry and Biochemistry, Mendel University in Brno, Zemedelska 1, CZ-613 00 Brno, Czech Republic

*Corresponding Author: parvez.mahbub@vu.edu.au

Abstract

Organic peroxide explosives (OPEs) are unstable, non-military, contemporary security threats often found in improvised explosive devices. Chemiluminescence (CL) can be used to detect OPEs, via radical formation consisting of peroxide moieties (-O-O-) under acidic conditions. However, selectivity for specific OPEs is hampered by the ubiquitous background of H_2O_2. Herein, we report the differentiation of hexamethylene triperoxide diamine (HMTD), triacetone triperoxide (TATP), and methyl ethyl ketone peroxide (MEKP) by specific flow injection analysis–CL (FIA-CL) signal profiles, after H_2SO_4 treatment. The radical degradation pathway of each structure, and its corresponding FIA-CL profile, was explored using mass spectrometry to reveal the rapid loss of -O-O- from TATP and HMTD structures, while MEKP formed CL signal-sustaining oligomers, as opposed to the immediate attenuation of H_2O_2. The CL response for OPEs in an aqueous media, measured via the described FIA-CL method, enabled ultra-trace limits of detection down to 0.40 µM for MEKP, 0.43 µM for HMTD, and 0.40 µM for TATP (combined linear range 1-83 µM with 95% confidence limit, n = 12). Expanded uncertainties of measurement (UM) of MEKP = ±0.98, HMTD = ±1.03, and TATP = ±1.1 (UM included probabilities of false positive and false negative as well as standard deviations of % recoveries and limit of detections of OPEs). Direct aqueous sample introduction via FIA-CL thus offers the prospect of rapid and selective screening of OPEs in security-heightened settings (e.g., airports), averting false positives from more ubiquitous H_2O_2.

Keywords: Acid hydrolysis, direct flow injection analysis-chemiluminescence, hydrogen peroxide, organic peroxide explosives, rapid screening, selectivity

44 **Introduction**

45 Organic peroxide explosives (OPEs) are a special class of explosives not used for military purposes
46 due to their highly unstable state. OPEs, such as hexamethylene triperoxide diamine (HMTD) and
47 triacetone triperoxide (TATP), can be synthesized in 'home laboratories'[1]. Crude synthesis of
48 OPEs has been possible because their ingredients, including mineral acids (e.g. nitric, sulfuric or
49 hydrochloric acids), acetone, and hydrogen peroxide (H_2O_2), are easily accessible. This along with
50 their rapid and simple synthesis has prompted exploitation of OPEs in several public
51 incidences[2]. OPEs are often chosen for such activities because HMTD and TATP achieve near
52 military-grade detonation velocity, calculated as 60% and 88% of the velocity of 2,4,6-trinitro
53 toluene, respectively[3]. Methyl ethyl ketone peroxide (MEKP), an emerging OPE, is also claimed
54 to achieve 51% detonation velocity compared to ammonium nitrate explosives[4]. Considering
55 their explosivity and illegal use in public places, rapid screening and selective detection of OPEs
56 is highly important.

57 One issue that inhibits the selective detection of OPEs via chemiluminescence (CL) is the presence
58 of a ubiquitous "background" H_2O_2, originating from household products such as hair dyes and
59 nail polish remover. This ubiquitous signal poses the risk of false positives during the rapid
60 screening process. All OPEs contain the peroxy -O-O- moiety, originating from the H_2O_2 utilized
61 in their synthesis. The instability of the -O-O- bond within an OPE structure presents a challenge
62 when attempting to differentiate an OPE signal from background H_2O_2 in a rapid screening
63 scenario; a currently unresolved concern. Krivitsky *et al*. (2019) have reported electrode sensing
64 of OPE vapor from collected air, unhindered from background H_2O_2[5]. However, it was noted
65 that at H_2O_2 concentrations beyond 150 ppm (4.4 mM) generate peaks at the same voltages as

66 TATP and HMTD, raising the possibility of false positives at the higher concentrations of H_2O_2 that
67 are expected from household products. To account for the potential broad range of H_2O_2 that
68 can be found in security settings, research on developing rapid and selective OPE screening is
69 warranted.

70 Several degradation mechanisms of H_2O_2 in aqueous solutions (e.g., acid/base hydrolysis,
71 photolysis, redox and enzymatic degradation) could be employed to eliminate the interference
72 of background H_2O_2. Of these, acid hydrolysis is the simplest and most inexpensive approach that
73 could be incorporated into a microfluidic system for interference-free OPE screening. Therefore,
74 we initially demonstrated a new screening approach for OPEs in aqueous samples, which involved
75 acid hydrolysis to differentiate OPEs from background H_2O_2. Following this, we developed a new
76 analytical method via flow injection analysis-CL (FIA-CL), which enabled ultra-trace detection of
77 OPEs in a time-sensitive manner without onerous sample preparation compared to conventional
78 detection methods.

79 Conventional detection of OPEs has included electrochemical[5, 6], acid-hydrolysis[7],
80 photolysis[2] , and reverse phase high performance liquid chromatography-Fourier transform
81 infrared (RP HPLC-FTIR)[8]. Additionally, surface-assisted laser desorption/ionization-time of
82 flight-mass spectrometry (SALDI-TOF-MS) and direct analysis in real time (DART-MS) were
83 employed in analyzing liquid OPE samples spread on ceramic tiles[9]. For liquid OPE samples
84 collected on vendor supplied polytetrafluoroethylene filters, ion mobility -tandem mass
85 spectroscopy (IM-MS/MS) was employed [10]. The analysis time, as is typically required by these
86 classical methods, varies between 1 and 30 min, with most requiring large laboratory-grade
87 instrumentation, arduous sample preparation, and analytes in volatile/aerosol forms, which may

limit their availability in many on-site investigations [11]. Conversely, solid OPE samples were analyzed by stand-alone IMS with a built-in Faraday plate electron capture detector, reported by Oxley and co-workers[12]. The IMS systems were reported to facilitate fast analysis time (<7 sec)[13], but the sample preparation time might take up to 16 days for specific OPEs (e.g., TATP) in explosive-mode (E-mode or negative IMS mode), mainly due to low detection sensitivity and high detection limit or LOD (3.9 μg for TATP) in E-mode[12]. In fact, the reported LODs of TATP (0.8 μg) in the studies of Oxley et al. (2008), were achieved in narcotics-mode (N-mode or positive IMS mode) through (1) placing human hair directly into the IMS desorption chamber, (2) swabbing hair with a sample trap and its subsequent placement within the vapour desorption unit, and (3) adding acetonitrile extract of hair to sample trap and then sample trap to desorption unit[12]. Ideally, during a rapid screening scenario, a swab is preferable to placing bodily components into the IMS desorption unit. This together with the high vapor pressures of many OPEs exacerbate the problem of an increased LOD for trace residual OPEs on a surface, due to their rapid volatilization in ambient air. Additionally, the selection of positive or negative ion modes in IMS appears to be a limiting factor in controlling the sensitivity and detection limits of OPEs via IMS. For example, whilst TATP was reported to be detected only in positive mode[12, 14], HMTD was shown to be determined in both positive and negative modes. Recently, HMTD was reported to form only negative product ions in the IMS's drift tube, thereby, acquired in negative detection modes[15]. This, together with a conventional screening system's inability to directly analyse aqueous OPE samples and a reliance on onerous sample preparation prior to their transfer to a costly thermal desorber[16, 17], demands an alternative screening system for OPEs.

110 OPEs are highly sensitive to impact, friction, and temperature change[18], readily releasing
111 compounds with unstable peroxy moieties (e.g. unstable $C_3H_6O_2$ isomers from TATP)[19], that
112 are detectable at trace levels in various sample matrices via the conventional analytical methods
113 previously mentioned. In these contexts, rapid microfluidic detection systems such as FIA-CL, that
114 negate selecting negative/positive modes, presents one of the fastest, most portable, and widely
115 employed analytical applications [20] for direct (without sample preparation) detection of OPEs
116 in aqueous solutions. Previous studies focused on indirect OPE detection (measuring the
117 concentration of released H_2O_2) via acid hydrolysis and photolysis[2, 7], involved lengthy sample
118 preparation. To date, direct detection of OPEs (i.e. *in situ* without sample preparation) in aqueous
119 forms via a portable microfluidic platform has not been reported. Therefore, in this study, we
120 present the development of a rapid and selective approach of differentiating OPEs from residual
121 H_2O_2 via acid hydrolysis, aiming towards their subsequent direct detection (in case of a positive
122 screening result of OPE) in aqueous forms via FIA-CL without onerous sample preparation.

123 **Materials and Methods**

124 **Chemicals and Consumables**

125 Analytical grade chemicals were used throughout. 30% (w/w) H_2O_2 was purchased from Sigma
126 Aldrich, Australia. Acids were selected based on gradually lower acid dissociation constants. HPLC
127 grade 98% sulfuric acid (H_2SO_4), nitric acid (HNO_3), acetic acid (CH_3COOH) and lactic acid ($C_3H_6O_3$)
128 were purchased from Sigma Aldrich, Australia. OPE standards (99.9% HMTD and TATP in
129 acetonitrile) were obtained from AccuStandard, USA, and MEKP was purchased from Sigma
130 Aldrich, Australia. Various oxidizers/reducers such as potassium permanganate ($KMnO_4$),

131 potassium dichromate ($K_2Cr_2O_7$), orthoperiodic acid (H_5IO_6), L-ascorbic acid ($C_6H_8O_6$), and
132 potassium iodide (KI) were purchased from Sigma Aldrich, Australia. More information about CL
133 agents and CL assay preparation are given in supplementary information (**Table S1**). The
134 fluoroethylene polymer (part no. 1677L) tubing and accessories (e.g., nuts and ferrules) to
135 construct the microfluidic FIA-CL system were purchased from Idex Health and Science, USA.

136 **Instrumentations**

137 A Hamamatsu head-on photomultiplier tube (PMT) was employed for CL measurements. The
138 PMT housed a built-in power supply circuit and a low noise amplifier (H7827-001, Japan) with
139 maximum emission sensitivity at ~430 nm wavelength. The circular CL reaction flow cell (CNC
140 milled; 2 mm nominal depth) was sealed with precision-cut quartz glass, having 99%
141 transmittance of the visible wavelength. A powerchrom data acquisition unit (eDAQ Pty Ltd.,
142 Sydney, Australia), installed with a powerchrom software (version 2.8.3), was employed for
143 analyzing the PMT data. A Rheodyne manual injector (6 port 2 position Make-Before-Break
144 (MBB™) Model 7725i, Merck Pty Ltd., Sydney, Australia) was connected to a peristaltic pump and
145 used as an automated sample loader. Fluid propulsions were regulated in a pulse-free manner
146 by micro-pressure regulators (IR 1000-01, SMC Corporation, Japan), which were connected to
147 500 mL Schott glass bottles via pneumatic tubing (6 mm ID, SMC Japan). Liquid flow rates were
148 precisely monitored with a Sensirion electronic microfluidic flow meter (SLI-1000-FMK, Sensirion
149 AG, Switzerland). A schematic representation of instrumentations is shown in **Figure 1**.

150

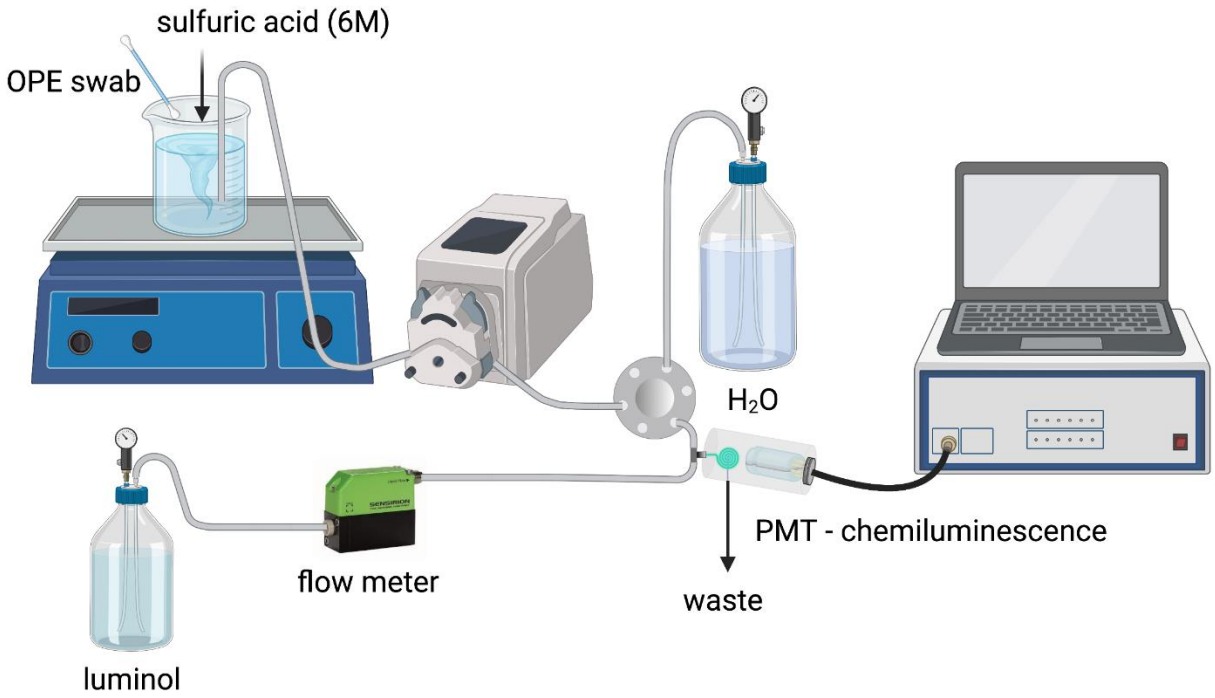

Figure 1. Schematic of rapid and selective screening of OPEs via FIA-CL platform showing the addition of sulfuric acid in a flow system as a rapid screening step that differentiates the chemiluminescence of luminol via release of peroxy moieties from OPEs from that of ubiquitous H_2O_2. PMT= photomultiplier tube. Known concentrations of OPEs on pig skins were deposited and swabbed from the skin surface within 10 min of deposition. Swabs were dipped in 200 mL deionised water. The FIA-CL method has two steps: 1. Rapid and selective differentiation of OPEs from H_2O_2 by comparing initial peaks without acid with subsequent peaks with acid, and 2. In case of a positive screening result of OPE, quantitation of OPE via analysing the initial peaks without acid from step 1. For optimal composition of CL assay, please refer to Table S1 in the supplementary information.

FIA-CL method of screening and selective differentiation of OPEs

The aim of this study was to understand the screening and differentiation of OPEs from H_2O_2 using FIA-CL as a suitable microfluidic platform. As Figs. 2-4 were focused on understanding the principles of differentiating OPEs from H_2O_2 during acid hydrolysis, equal concentrations of OPE

166 and H_2O_2 (~9-10 µM) hydrolysed by 6 M H_2SO_4 were injected into the FIA-CL system following the
167 parameters given in Table 1. The experiment described in Fig. 5 aimed to illustrate the effect of
168 dissociation constants of different acids on the degradation of OPE. Hence, in Fig. 5, 2.5 µM MEKP
169 hydrolysed by 1 M of various acids were injected. In our effort to illustrate the determinative step
170 in case of a positive OPE screening result, the experiment in Fig. 8 demonstrated whether a single
171 swab loaded with OPE from a model skin surface can quantitatively detect OPEs or not. Hence,
172 in Fig. 8, 10 µL 30 mM OPEs were swabbed within 10 minutes of deposition on 25 mm x 25 mm
173 cut of pig skins and dipped into 200 mL DI water blank, followed by injection into the FIA-CL as
174 per the optimised parameters of Table 1.

175 The CL line of Fig. 1 (i.e., line connecting luminol bottle to PMT) was fitted with the flow meter,
176 and hence the flow rate in this line was precisely measured and observed on the computer
177 screen. The carrier line of Fig. 1 (i.e., line connecting H_2O bottle to PMT) did not have a flow
178 meter, and hence flow rate in this line was only controlled via the SMC pressure regulators. For
179 optimum performance of both pressure regulators, we maintained a constant 60 psi building
180 pressure (termed as regulated back pressure) at the inlet. We aimed to maintain a rapid analysis
181 time (<60 sec from injection to detection) and found that 20 psi in CL line and 50 psi in carrier
182 line resulted reproducible peaks within ~30 sec of the injection. For this FIA set-up, the CL line
183 showed a flow rate of 250 µL min^{-1} via the flow meter. For maximum reproducible peak intensity,
184 we employed the similar CL assay used in our previous FIA-CL studies [2, 7]. Table 1 provides the
185 FIA-CL operating conditions.

186 Table 1: Optimised operating conditions of the FIA-CL system for selective OPE detection (Fig. 1).
187 Abbreviations: internal diameter (ID); outside diameter (OD).

FIA-CL parameter	Optimisation range tested	Final optimal value
Sample loop	20 - 100 µL	40 µL
CL line (ID)	1.5- 2 mm	1.5 mm
CL line (OD)	3 mm	3 mm
Carrier line (ID)	1.5- 2 mm	1.5 mm
Carrier line (OD)	3 mm	3 mm
CL pressure	20-40 psi	20 psi
Carrier pressure	20-50 psi	50 psi
Regulated back pressure	60 -100 psi	60 psi
PMT gain range	980- 1000 mV	986 mV
CL flowcell	2 mm ID; 1 mL nominal volume	2 mm
Pneumatic line (ID)	6 mm	6 mm
Fixed assay conditions		
CL assay	luminol (0.51 mM) and cobalt chloride (9.96 µM $CoCl_2.6H_2O$) in aqeous media with $Na_2HPO_4.7H_2O$ (50 mM) and NaOH (40 mM)	
Carrier media	Millipore 18.2 MΩ cm at 25 °C deionised water	

188

189 **Characterization of Acid Degradation Products of OPEs**

190 The acid degradation products of OPEs were investigated by direct sample analysis-time of flight
191 mass spectrometry (DSA-TOF MS), which consisted of a mass spectrometer (AxION2 TOF MS,
192 Perkin Elmer, USA) coupled with an ionization source (AxION® DSA™, Perkin Elmer, USA).
193 Acquisition parameters were set at 10 spectra/s, pulsed, in positive mode. Ion source voltages
194 included: needle 2000 V, endplate 200 V, and capillary 800 V. The drying gas flow rate was
195 maintained at 3 L min^{-1}. Nitrogen was used as the ionization gas for all DSA-TOF MS experiments,
196 and the atmospheric pressure chemical ionization (APCI) heating temperature was set to 220 °C.

197 The mass spectra for OPEs were collected in full scan acquisition mode (m/z 50 – 2000). APCI-L
198 low concentration tuning mix (G1969-85010, Agilent Technologies) was employed for DSA
199 calibration. Initially, 5 µL of OPEs (1 µM), prepared in ultrapure water (UPW), was deposited on
200 the sample mesh of DSA-TOF-MS to observe their mass spectral signature. Then, 1 µL of
201 concentrated OPEs (1:4 v/v OPE standard: UPW) was placed on the sample mesh, followed by 1
202 µL of concentrated OPEs in 3.25 µL UPW and 0.75 µL 6M H_2SO_4.

203 Desorption ionization on silicon (DIOS) TOF MS (Ultraflextreme, Bruker, Germany) was also
204 employed to confirm the acid degradation products of OPEs. The DIOS surface was fabricated in-
205 house at the Melbourne Centre for Nanofabrication (MCN)[21]. After calibration of the
206 instrument with cesium iodide clusters[21], acquisition was obtained in reflectron positive mode
207 using a 1 KHz Smartbeam™-II laser, with a 100 µm laser diameter, collecting 1000 shots @ 1000
208 Hz in a random walk pattern. Spectra were collected in the 40 - 3500 Da range. For DIOS TOF MS,
209 initially, 0.2 µL of standard OPE sample was deposited on the DIOS surface. Then, 1 µL of
210 concentrated OPEs was spiked with 1 µL 6M H_2SO_4. From this mixture, 0.2 µL of aliquot was
211 placed directly on the DIOS surface for MS analysis.

212 **Results and Discussions**

213 Since H_2O_2 could be potentially present in an OPE screening environment, we initially determined
214 residual H_2O_2 concentration on cotton (shirt), pig skin, acrylic (false nails), and synthetic human
215 hair; mimicking possible areas where H_2O_2 contamination might be present. Swabs of 6%
216 household H_2O_2 from these surfaces revealed that pig skin elicited the most reproducible FIA-CL
217 signal, compared to other models (**Figure S1**). Residual H_2O_2 recovery from swabs (maximum

218 value estimated to be 79 ± 1.4%) were then tested by spiking the sterile polystyrene surface with
219 10 µL household 6% H_2O_2 (**Figure S3**). Its recovery efficiency of H_2O_2 for other surfaces is shown
220 in **Table S2**. As background H_2O_2 may interfere with direct OPE detection, we focused on
221 eliminating this using various oxidizing/reducing agents, namely potassium permanganate
222 ($KMnO_4$), potassium dichromate ($K_2Cr_2O_7$), orthoperiodic acid (H_5IO_6), ascorbic acid ($C_6H_8O_6$), and
223 potassium iodide (KI) (**Figure S4 & S5**). The intent was to conduct a selective analysis to
224 differentiate OPEs from background H_2O_2. Our results indicated that neither of these
225 oxidizers/reducers met that purpose (**Figure S6)**. This led us to employ acid hydrolysis as a
226 selective screening approach to differentiate OPEs from H_2O_2. A direct FIA-CL approach to rapidly
227 detect OPEs, without onerous sample preparation, would be more fitting with screening in a
228 security environment, and amenable to miniaturization into a microfluidic system.

229 **Distinguishing H_2O_2 from the OPEs**

230 Initially, the decomposition of H_2O_2 in the presence of H_2SO_4 was investigated. The addition of
231 H_2SO_4 to H_2O_2 caused degradation of H_2O_2 and resulted in incomplete reaction between its
232 degradation products and luminol, as evident in the broadening of the peaks (heights of peaks 4-
233 6 compared to those of peaks 1-3), as shown in **Figure 2**. Such broadening of the peaks was due
234 to the decreasing pH level (pH 2.52 upon addition of H_2SO_4) in the FIA-CL system. The low level
235 of pH was probably responsible for an incomplete chemiluminescence (CL) reaction in the system
236 (as opposed to optimal pH level of ~9-11), which was confirmed by our previous study [7],
237 reporting the pH dependence of CL reaction between H_2O_2 and luminol. It was further stated that
238 the CL signals markedly reduced at pH 8, showing no signal at pH 2.5[7]. The slight increase in the
239 signals of peaks 1-3 from 3 consecutive injections of 10 µM H_2O_2 in Fig. 2 might have resulted due

240 to instantaneous fluctuation in flow regime during injection via the manual injector, although
241 such minor fluctuations do not affect the measurement as long as the relative standard
242 deviations (RSDs) of signals were within acceptable limits for analytical measurement (Burrows
243 and Parr 2020) [22]. Additionally, we emphasize that Fig. 2 is intended towards finding
244 differentiating phenomena during acid hydrolysis of H_2O_2, rather than quantitation of H_2O_2.
245 Hence, the increase in peak heights 1-3 in Fig. 2 did not affect our investigation of finding the
246 differentiating phenomena. For quantitative analyses, please see our discussions of Fig. 8 later in
247 the 'Direct Detection' section. Additionally, we maintained a constant gain (i.e., output voltage)
248 of PMT and almost equal and comparable concentrations of OPE and H_2O_2 (~9-10 µM) in our
249 attempt to find the differentiating phenomena amongst these substances in Figs. 2-4.

250

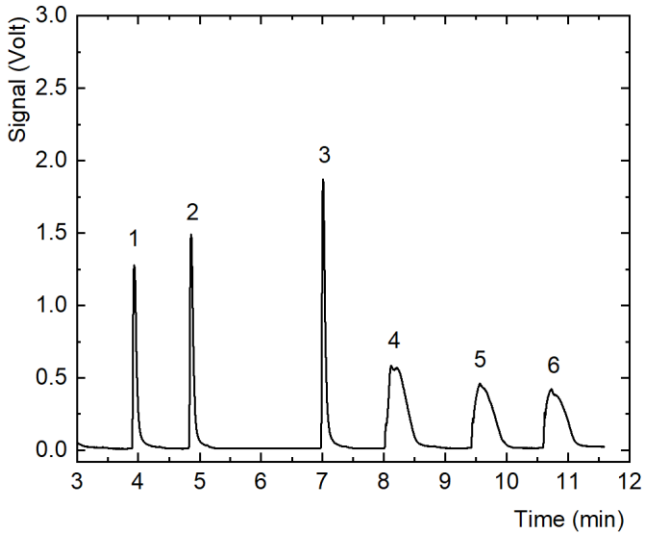

251

252 **Figure 2.** Showing attenuation of chemiluminescence signal intensity (average signal to noise or
253 S/N of peaks 4-6 = 0.5 V ± 0.05) following spiking H_2O_2 (200 mL of 10 µM) with H_2SO_4 (50 µL of
254 6M) compared to signal intensity without H_2SO_4 (average S/N of peaks 1-3 = 1.6 V ± 0.3).
255 [injection volume: 40 µL, flow rate: 250 µL min^{-1} in CL line, pressure: 20 psi in CL line and 50 psi

256 in carrier line; CL assay: 0.51 mM luminol + 9.96 µM $CoCl_2.6H_2O$ in 50 mM $Na_2HPO_4.7H_2O$ and 40
257 mM NaOH buffer]. Approximately 7.3 fold broadening of peaks 4-6 (full width at half maxima or
258 FWHM = 0.58 ± 0.08 min) resulting from acid hydrolysis of H_2O_2 as compared to peaks 1-3 (FWHM
259 =0.08 ± 0.002 min)

260 Notably, on the addition of H_2SO_4 (50 µL of 6 M), MEKP generated sustained and saturated
261 luminescence signals, reaching the maximum voltage limit coming from the PMT detector (peaks
262 4, 5 with H_2SO_4 compared to peaks 1-3 without H_2SO_4) (**Figure 3**). The signal response returned
263 to original peak intensity on removal of H_2SO_4 (peaks 6-8 in **Figure 3**). A similar saturated signal
264 was achieved even when a 2-fold reduction of volume of H_2SO_4 was applied, indicating release of
265 peroxy (-O-O-) moieties either from direct degradation or from oligomeric derivatives of OPEs,
266 which can form through hydrolysis and acid condensation/polymerization (**Figure 4;** volume of
267 6M H_2SO_4 down to 25 µL from 50 µL as in **Figure 3**). The acid-catalyzed (e.g. using H_2SO_4) stepwise
268 degradation pathway of OPEs, marked by the release of H_2O_2 and acetone, was proposed by
269 Armitt *et al*. (2008)[23]. This proposition is also supported by Tsaplev (2012)[24], reporting that
270 the rate of active oxygen (i.e. H_2O_2) formation from TATP increased with increasing acid
271 concentrations, which was more prominent in H_2SO_4 than in HCl.

272

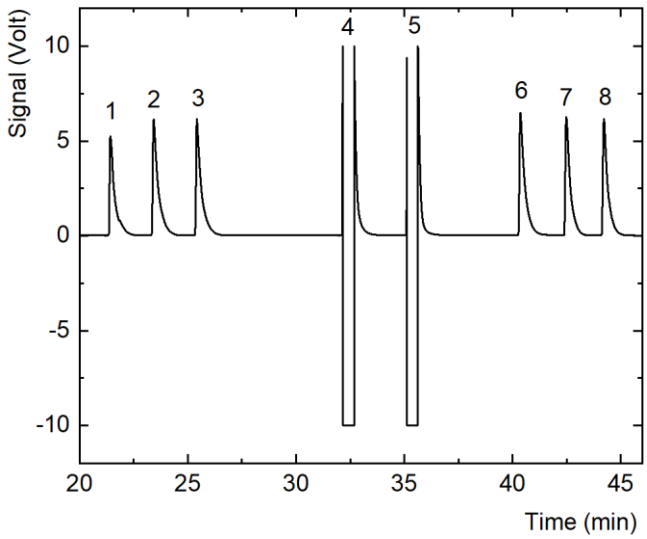

Figure 3. Effect of acid hydrolysis on MEKP (peaks 1-3: 10 µM MEKP with average peak signal to noise or S/N= 6.1 ± 0.4 volts, peaks 4-5: 10 µM MEKP after H_2SO_4 treatment resulting signal saturation), showing remarkable increase in signal intensity exceeding the FIA-CL detector's capacity due to the release of peroxy moieties from MEKP, and peaks 6-8 (average S/N = 6.3 ± 0.01 volts) returned to normal peak intensity when H_2SO_4 was removed. The relative standard deviation (RSD %) of six MEKP peaks (i.e., 1-3 and 6-8) = 4.2%, which is well within the acceptable RSDs at ppb level of analyte concentrations [25]. [injection volume: 40 µL, volume of 6M H_2SO_4: 50 µL, flow rate: 250 µL min^{-1} in CL line, pressure: 20 psi in CL line and 50 psi in carrier line; CL assay: 0.51 mM luminol + 9.96 µM $CoCl_2.6H_2O$ in 50 mM $Na_2HPO_4.7H_2O$ and 40 mM NaOH buffer].

Conversely, it was interesting to note how the CL signal intensity changed when lower concentrations of H_2SO_4, along with nitric acid (HNO_3), acetic acid (CH_3COOH), and lactic acid ($C_3H_6O_3$) were used. Noticeably, lowering acid concentrations from 6 M (**Figure 4**) to 1 M (**Figure 5**) not only increased the pH value in the FIA-CL system, but also enabled overall sharper peak shapes with reduced peak tailing and splitting (as compared to **Figure 4**). Such signal behavior of the system also indicated more complete CL reactions.

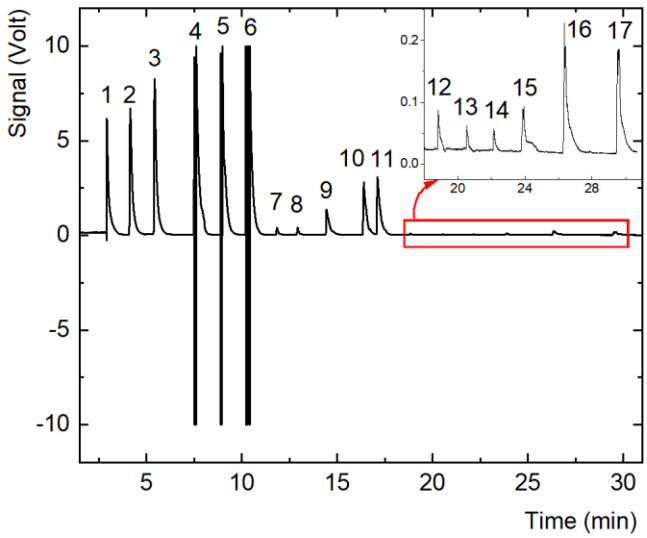

Figure 4. Consistent boost of signal intensity when treating OPEs by H_2SO_4 with a 2-fold reduction in the volume of acid used. Peaks 1-3: 10 µM MEKP (average signal-to noise or S/N 7.1 ± 1.1 volts), peaks 4-6: 10 µM MEKP after H_2SO_4 treatment resulting signal saturation as in Fig. 3, peaks 7-8: 9.6 µM HMTD (average S/N 0.51 ± 0.01 volts, FWHM = 0.351 ± 0.001 min), peaks 9-11: 9.6 µM HMTD after H_2SO_4 treatment (FWHM = 0.95 ± 0.05 min, thus acid hydrolysis resulting ~2.7 fold HMTD peak broadening compared to peaks 7-8), peaks 13-14: 8.9 µM TATP (average S/N 0.071 ± 0.001 volts, FWHM = 0.32 ± 0.01 min, and peaks 15-17: 8.9 µM TATP after H_2SO_4 treatment (FWHM = 0.55 ± 0.04, thus acid hydrolysis resulting ~1.72 fold TATP peak broadening compared to peaks 13-14]. [injection volume: 40 µL, volume of 6M H_2SO_4: 25 µL, flow rate: 250 µL min^{-1} in CL line, pressure: 20 psi in CL line and 50 psi in carrier line; CL assay: 0.51 mM luminol + 9.96 µM $CoCl_2.6H_2O$ in 50 mM $Na_2HPO_4.7H_2O$ and 40 mM NaOH buffer].

Observing the peaks in Figs. 4, we emphasize that in our attempt to find the differentiating phenomena during acid hydrolysis of OPEs, the on and off acid-intervention into the system in Figs. 4 might have resulted pH fluctuations in the system, thereby affecting the resulting peak heights and shapes of OPEs. Nevertheless, Figs. 2 -4 established the differentiating phenomena during acid hydrolysis (i.e., signal boost in case of OPEs and signal attenuation in case of H_2O_2).

310 The dissociation constant values of acids (pK_a) had a pronounced effect on protonating the MEKP
311 structure and its consequent release of peroxy moieties, which is observed in Fig. 5 through the
312 gradually reduced signal intensities starting from 1 M H_2SO_4 (pK_a = -10.0) and ending with 1 M
313 CH_3COOH (pK_a = 4.75). **Figure 5** further indicated that no other acids except H_2SO_4 were found to
314 be capable of differentiating the residual H_2O_2 peaks from that of OPEs. Such differentiation was
315 evident when 1 M of H_2SO_4 was added to the OPE samples, releasing significant amount of
316 H_2O_2/derivatives containing peroxy moieties from this OPE structure and causing an increase of
317 the peak signals unlike nitric (HNO_3), lactic ($C_3H_6O_3$) or acetic (CH_3COOH) acids. Acetic acid's
318 inability to degrade OPEs (e.g. TATP) was also observed by Armitt *et al*. (2008)[23]. Additionally,
319 as acid hydrolysis continuously progresses within each sample that were repeatedly injected, the
320 'not so good' repeatability of the peaks in Fig. 5 (e.g., amongst peaks 3-5, or amongst peaks 6-7
321 and so on) is expected after the start of acid treatment. From the above discussion, we propose
322 that H_2SO_4 can be employed for selective differentiation of OPEs from residual H_2O_2.

323

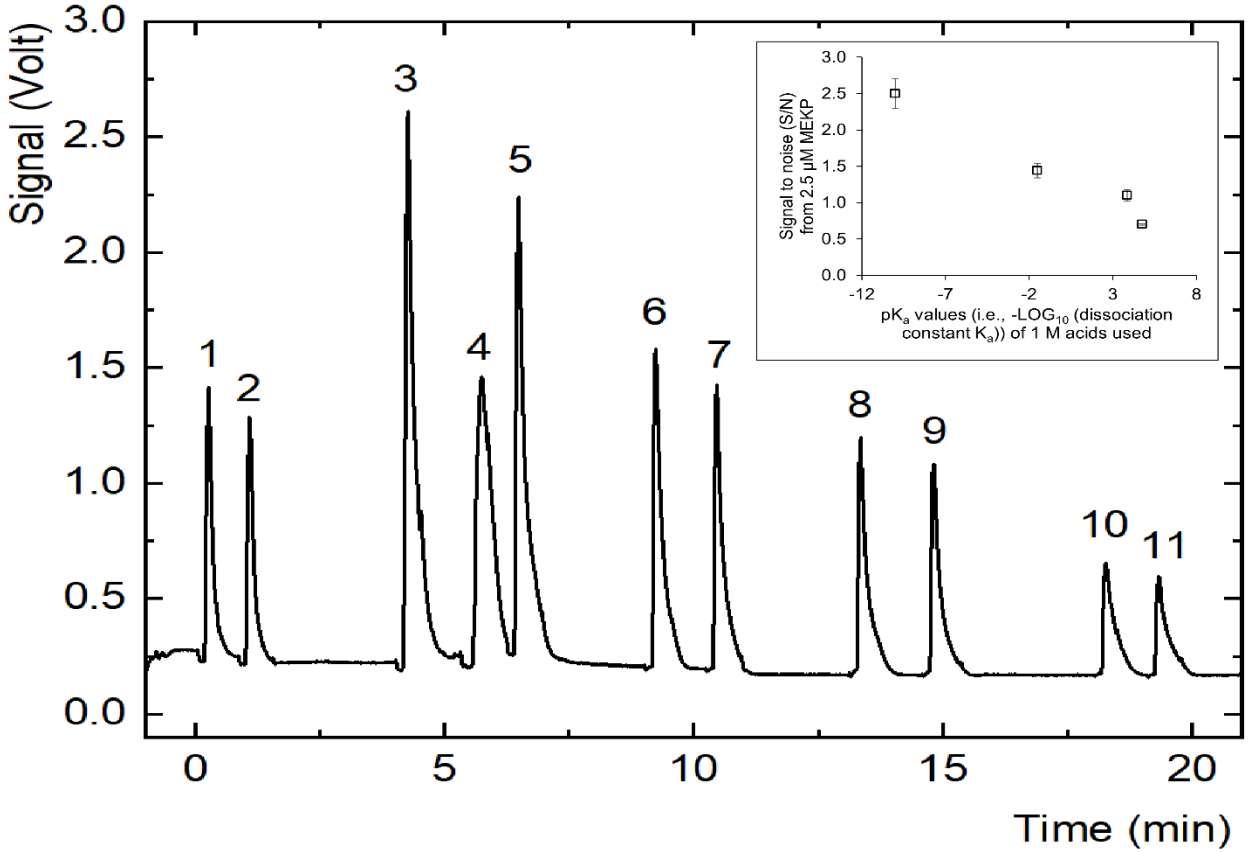

324

325 **Figure 5.** Comparison of signal intensities when MEKP (2.5 µM) treated with 1 M acids with
326 gradually reduced acid dissociation constant values. [peaks 1-2: without acid treatment, peaks 3
327 -5: after H_2SO_4 treatment (pK_a = -10.0), peaks 6-7: after HNO_3 treatment (pK_a = -1.5), peaks 8-9:
328 after $C_3H_6O_3$ treatment (pK_a = 3.86), peaks 10-11: after CH_3COOH treatment (pK_a = 4.75)].
329 [injection volume: 40 µL, volume of acids: 10 µL each, flow rate: 250 µL min^{-1} in CL line, pressure:
330 20 psi in CL line and 50 psi in carrier line; CL assay: 0.51 mM luminol + 9.96 µM $CoCl_2.6H_2O$ in 50
331 mM $Na_2HPO_4.7H_2O$ and 40 mM NaOH buffer]. The gradual increase in the degree of acid
332 hydrolysis of 2.5 µM MEKP via utilizing stronger acids is shown in the inset.

333 **Acid Condensation Polymerization of OPEs**

334 To understand how each OPE generates a specific chemiluminescence profile, and hence
335 generates selectivity in the FIA-CL response, we used mass spectrometry to determine the effect
336 of H_2SO_4 on OPE structure. DSA-TOF-MS detected both MEKP and HMTD, as well as their H_2SO_4
337 acid degradation products. When H_2SO_4 was applied to MEKP, a MEKP dimer was detected at
338 m/z 199.2086 as well as higher order oligomers such as, trimer at m/z 287.2769, tetramer at m/z
339 322.5292, pentamer at 503.4861, and a Na^+ adduct ion of hexamer at m/z 583.4478 (**Figures 6a-**
340 **b**). The formation of MEKP's oligomers via acid condensation polymerization in acidic
341 environment has been previously reported by Milas and Golubovic (1959)[26] and Yuan *et al*.
342 (2005)[27]. All these oligomers of MEKP contain multiple numbers of peroxy (-O-O-) moieties,
343 and higher order MEKP oligomers contain more peroxy moieties than the lowers order oligomers.
344 The chemiluminescence (CL) reaction in our proposed FIA-CL approach is a cobalt catalysed
345 luminol CL reaction with maximum emission at 425 nm. Burdo and Seitz (1975) [28]have reported
346 that a cobalt- H_2O_2 complex is the essential Intermediate required for cobalt catalysed luminol
347 CL. As (-O-O-) moieties are common in MEKP acid-hydrolysates as well as in H_2O_2, we expect
348 similar cobalt catalysed CL reactions between MEKP oligomers and luminol. Hence, the increased

presence of these peroxy moieties leads to more intense CL, thereby likely to contributing to the saturation of FIA signals as demonstrated in **Figure 4** (peak heights 4-6 compared to peaks 1-3). The DSA-TOF-MS analyses further revealed complete degradation of HMTD (m/z 209.1267) and its dialdehyde derivative tetramethylene diperoxide diamine dialdehyde (TMDDD) (m/z 207.1487)[29] into decomposition products[30], identified as $[C_3H_7ON+H]^+$ at m/z 74.097, [2(CHO)NH] at m/z 73.0735, and $[C_3H_2O+H]^+$ at m/z 55.0579 (**Figures 6c-d**). The release of the peroxy moiety (-O-O-) from the completely degraded HMTD and TMDDD during H_2SO_4 hydrolysis resulted in the sharp increase in FIA signals, as it was shown in **Figure 4** (peak heights 9-11 compared to peaks 7-8).

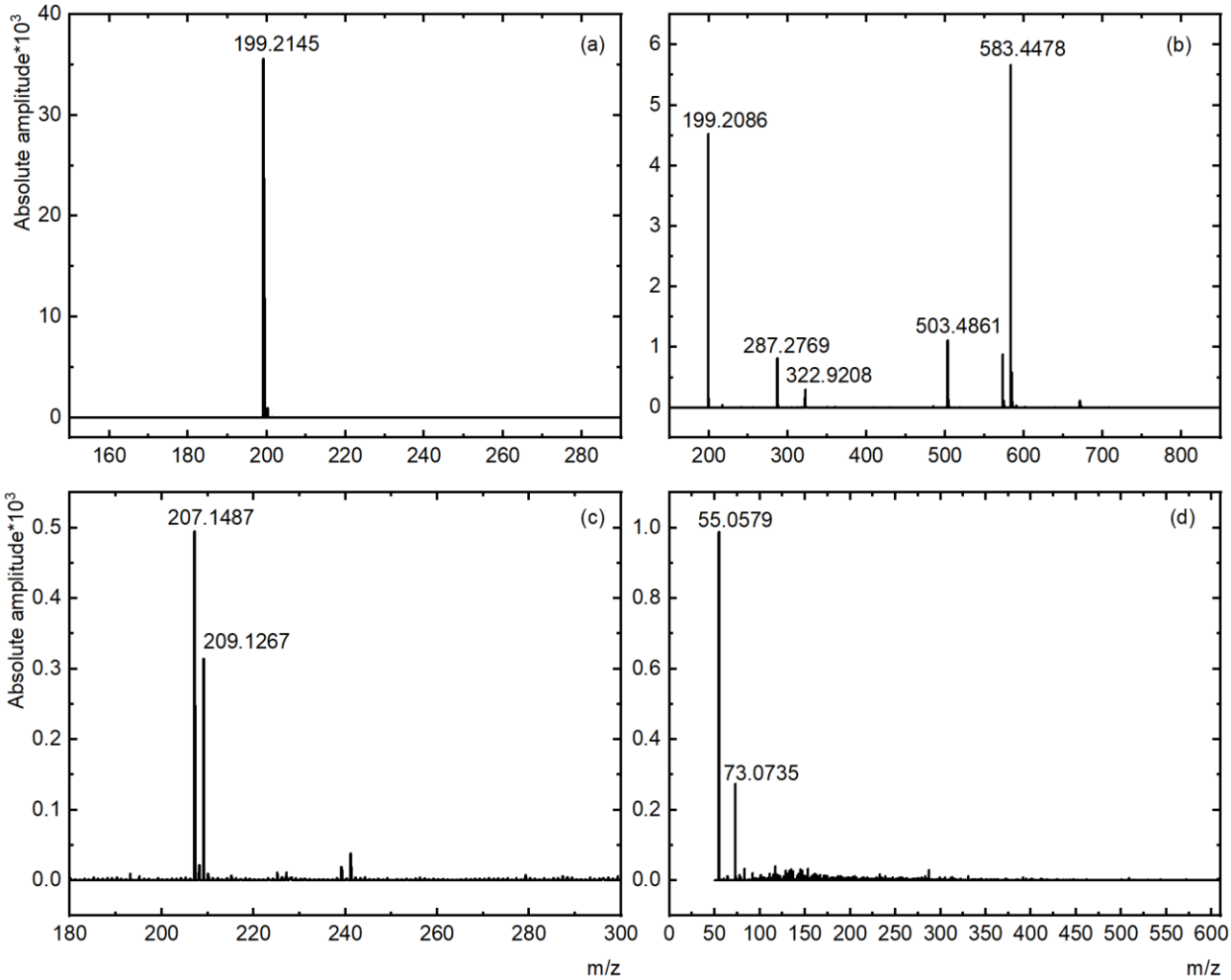

359 **Figure 6.** DSA-TOF mass spectra of OPEs with/without H_2SO_4 analyzed, (a) MEKP (1 µL of 30.2 µM
360 in ultrapure water (UPW), (b) MEKP (1 µL of 30.2 µM in UPW) spiked with H_2SO_4 (4 µL of 6M), (c)
361 HMTD (1 µL of 96.1 µM in UPW), and (d) HMTD (1 µL of 96.1 µM in UPW) spiked with H_2SO_4 (4
362 µL of 6M).

363

364 Employing DSA-TOF MS to analyze TATP appeared to provide inconsistent spectra. This is partly
365 related to TATP's high volatility at ambient condition because of its low vapor pressure of 4.65 x
366 10^{-2} Torr at 25 °C[31]. Hence, we employed an alternative mild ionization technique,
367 desorption/ionization on silicon (DIOS) TOF MS for detection and identification of TATP acid
368 degradation products, which allows partial trapping of the TATP sample into a nanoporous silicon
369 layer. DIOS TOF MS showed a TATP tetramer at m/z 298.417, following laser
370 desorption/ionization (**Figure 7a)**. The formation of a TATP tetramer ($C_{12}H_{24}O_8$) is also supported
371 by Jiang *et al*. (1999)[32], who reported the existence of a similar oligomer when acetone was
372 oxidized by 30% H_2O_2 in presence of tin (IV) chloride pentahydrate ($SnCl_4.5H_20$) as a catalyst. The
373 tetramer was found to further degrade into fragments when TATP was spiked with H_2SO_4 (**Figure**
374 **7b)**.

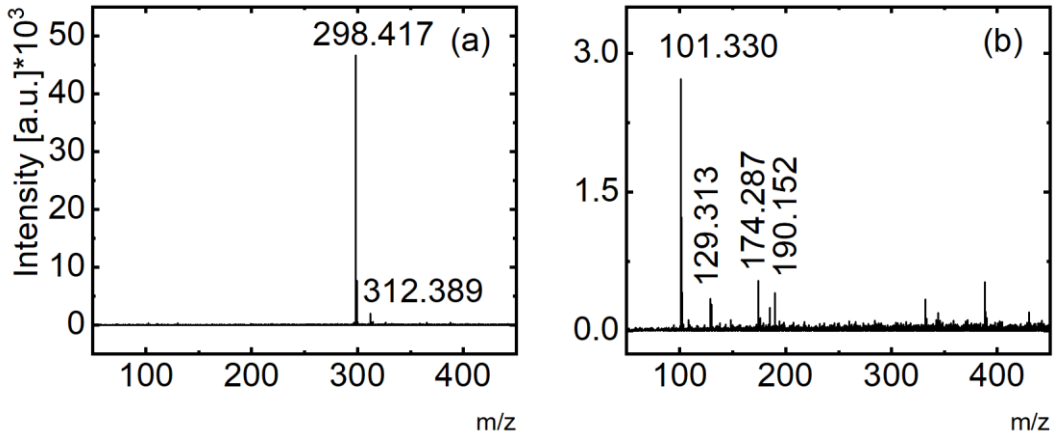

Figure 7. DIOS TOF mass spectra of TATP, (a) before (1 µL of 449 µM TATP) and (b) after spiking with H_2SO_4 (1 µL of 449 µM TATP + 1 µL 6M H_2SO_4).

These fragments correspond to the major moieties found in the TATP tetramer structure, for example, m/z 190 [M-CH_3COOCH_3- H_2O_2], m/z 174 [M-CH_3COOCH_3-H_2O_2-CH_2], m/z 129 [M-CH_3COOCH_3-CH_3COO-H_2O_2], and m/z 101 [M-CH_3COOCH_3-H_2O_2-CH]. The release of CH_3COOCH_3 from TATP, when exposed to H_2SO_4, agrees with the findings of Armit *et al* (2008)[23]. MS/MS analysis (**Figure S7**) of m/z 298 revealed the loss of CH_3COOCH_3 fragments from the tetramer, giving rise to moieties 2(CH_3)COO- at m/z 74.44, 2(CH_3)CO-H at m/z 56.793, and CH_2CO at m/z 42.512. The release of such moieties due to thermal decomposition of TATP matched with those described by Hiyoshi and Nakamura (2007)[33]. The release of these derivatives following spiking the TATP with H_2SO_4 confirmed the sharp rise in FIA-CL signal intensity, shown in **Figure 4** (peak heights 12-14 compared to peaks 15-17). Clearly, degradation of OPEs takes place in the presence of H_2SO_4, generating several of their oligomers, which trigger a structure specific FIA-CL signal, differentiating OPEs from background H_2O_2 and from each other.

Direct Detection of OPEs in FIA-CL System

391 After positively screening the OPEs from H_2O_2, the logical next-step would be their quantitative
392 detection via FIA-CL. We mentioned 'direct' to highlight the fact that in the event of a positive
393 screening result in the initial screening step, OPEs can be quantified without any further sample
394 injection and/or conventional sample preparation on a microfluidic platform. The initial OPE
395 signals without acid as detected in step 1 of the proposed FIA-CL approach can be employed for
396 OPE quantitation. If the result of rapid OPE screening is negative, then there will be no need for
397 their 'direct' detection. As mentioned in the supplementary information, pig skins being the
398 closest model to human skin, we swabbed known concentrations of OPEs from pig skins (25 mm
399 x 25 mm square pieces as shown in Fig. S2) in our attempt to analyse real samples. In this context,
400 we emphasize that a sample with both OPE and background H_2O_2 will boost the analytical signal
401 after acid hydrolysis as OPEs via either losing -O-O- moieties from HMTD and TATP, or via forming
402 a multiple number of CL signal-sustaining oligomers from MEKP as we have observed in Figs. 2-
403 4. However, such a sample cannot be used for OPE quantitation in the event of a positive
404 screening result of OPE, as FIA-CL will only produce a single resultant peak (from both OPE and
405 H_2O_2) per injection. Therefore, we only deposited known concentrations of OPEs on pig skins and
406 swabbed the surface of the skin within 10 min of deposition as part of our real sample analyses
407 in Fig. 8. We accept the fact that quantitation of OPEs will not be applicable via our proposed
408 method in case OPEs are present with H_2O_2 in the sample, although it will positively screen the
409 sample for OPE.
410 Herein, we present the FIA-CL analytical method to rapidly screen OPE samples and their
411 subsequent direct detection (in the event of a positive screening result) from the single swab,
412 allowing ultra-trace level of detection and achieving linearity (linear range 1 – 83 μM, $R^2 > 0.99$)

413 (**Table S3 & Figure S8**). Spontaneously released peroxide moieties from the OPE samples did

414 result in oxidation of luminol (**Figures 8a-c**), enabling such direct detection of OPEs.

415

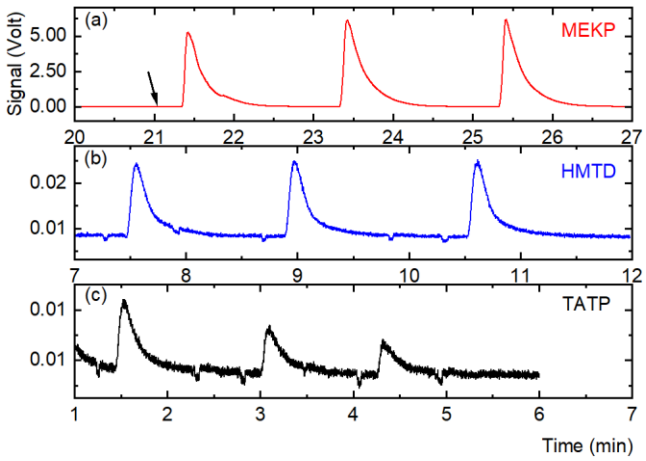

416

417 **Figure 8.** Direct detection of OPEs prior to acid hydrolysis in FIA-CL via injection of (a) MEKP (1.5

418 µM), (b) HMTD (1.5 µM), and (c) TATP (1.5 µM). Arrow indicates the sample injection time.

419 [Samples swabbed within 10 min of deposition of 10 µL 30 mM OPEs on pig skins and swab dipped

420 into 200 mL DI water blank, injection volume: 40 µL, flow rate: 250 µL min^{-1} in CL line, pressure:

421 20 psi in CL line and 50 psi in carrier line; CL assay: 0.51 mM luminol + 9.96 µM $CoCl_2.6H_2O$ in 50

422 mM $Na_2HPO_4.7H_2O$ and 40 mM NaOH buffer]. For % recovery of three OPEs, please see **Table S4**

423 in supporting information. Relative standard deviation (RSD %) of MEKP = 1.6%, HMTD = 0.2% ,

424 and TATP = 6% .

425 This direct detection scheme of OPEs via FIA-CL, as demonstrated in **Figures 8a-c**, has great

426 implications in any rapid *in situ* OPE screening mechanism as it is independent of any sample

427 preparation or pre-treatment. This would save significant amount of cost and time unlike

428 alternative OPE detection methods which rely heavily on onerous sample preparation. Another

429 important advantage of the developed approach is that it allows swabs to be inserted into a semi-

430 sealed, water interfaced FIA-CL system for OPE detection. Additionally, the system's analysis time

431 of ~12.5 s (from injection to start of peaks in **Figures 8a-c**) was close to an alternative rapid IMS
432 analytical time of ~7 s[12].

433 For comparison of available techniques, we present the LOD values of the current study along
434 with other detection methods published between 2016-2021 (see **Table 2**). The LOD values of
435 TATP and HMTD achieved via direct FIA-CL were found to be comparable or better than that
436 obtained with other detection methods. The FIA-CL method's LOD for MEKP (0.40 µM) was found
437 to be 1000 times lower than that achieved via direct-analysis-in-real-time ionization with mass
438 spectrometry (DART-MS)[34]. LODs for MEKP have yet to be reported for IMS systems to date.
439 Achieving LOD values of OPEs without acid hydrolysis clearly indicate that the FIA-CL system can
440 directly be employed for ultra-trace level detection of these explosives.

441 **Table 2.** Organic peroxide explosives (OPEs) detection methods published over the last six years
442 (2016-2021).

Name of OPEs	Sample type	Detection Method	LOD	Analysis time	Ref.
MEKP, HMTD & TATP	Aqueous	FIA-CL	MEKP (0.4 µM) HMTD (0.43 µM), & TATP (0.40 µM)	~12.5 s	This work
HMTD & TATP	Air	Electrochemical	<10 ppb	3 s	[5]
HMTD	Liquid	Dopant-assisted photoionization IMS	0.2-0.3 mg L^{-1}	10 s	[17]
HMTD & TATP	Aqueous	Electrochemical	HMTD (3.0 mg L^{-1}) TATP (1.5 mg L^{-1})	>5 min	[35]
TATP	Aqueous	Electrochemical	0.31 mg L^{-1}	>55 min	[36]
HMTD & TATP	Aqueous	LC-APCI-QToF-MS	HMTD (0.5 ng) TATP (10 ng)	4-8 min	[37]
HMTD & TATP	Gaseous	Electrochemical	HMTD (not reported) TATP (8.7 ng)	60 s	[38]
TATP	Gaseous	Electrochemical	40 ppb	60 s	[39]
TATP	Liquid	Colorimetry	0.1 mg L^{-1}	>11 min	[40]
HMTD	Liquid	Paper spray mass spectrometry	2.5 ng	0.5 min	[41]
HMTD	Liquid	DART-MS	Closed-mesh (250 ng) Direct insert (5 ng)	6-10 s	[42]
TATP	Liquid	Colorimetry	5.13 x 10^{-4} mol L^{-1} –	>17 min	[43]

3.54×10^{-7} mol L^{-1}

443

444 **Measurement Uncertainty**

445 As discussed earlier, the proposed FIA-CL method has two steps: 1. Rapid and selective
446 differentiation of OPEs from H_2O_2 by comparing initial peaks without acid with subsequent peaks
447 with acid, and 2. In case of a positive screening result of OPE, quantitation of OPE via analysing
448 the initial peaks without acid from step 1. Therefore, in our proposed method, quality control
449 and quality assurance (QA/QC) parameters for the detection (i.e., step 2) are always related to
450 that of screening (i.e., step 1) since only a single swab is proposed for both the steps. As in any
451 other analytical method, there is always a degree of uncertainty in the screening. The method's
452 uncertainty might be caused by 1. False positive, 2. False negative, 3. Reported limit of detection
453 (LOD) of OPEs in the study 4. Reported % recovery OPEs from the pig skin. The probability of 'false
454 positive' might occur if organic peroxides different from OPEs are present in the sample. Out of
455 7 different types totaling with a list of 151 organic peroxides (UNECE 2022)[44], the probability
456 of occurrence of an organic peroxide other than OPEs in the sample would be 1/151 = 0.007. The
457 probability of 'false negative' might occur in the case of expired CL assay, which will be very rare
458 as we proposed weekly replacement of the CL assay in our previous studies. We prepared
459 approximately 100 CL assay over 1 month period and only 1 of those assays expired before 7
460 days. Hence, in our case, monthly probability of occurrence of expired CL assay were 1/100= 0.01.
461 We have undertaken a 4-point calibration with three replications of each observation (Fig. S8 in
462 ESI), hence, there were 12 observations or samples in total. Therefore, Standard deviation (Stdev)
463 of 'false positive'= Square root (sample size * probability of occurrence * (1- probability of

occurrence)) = 0.29 and that of 'False negative' = 0.34. The standard deviations of LODs and percentage recoveries of OPEs were provided in Tables S3 and S4 of ESI, respectively.

The 'Expanded Uncertainty (U)' of the screening of OPEs would be expressed as (Taylor and Kuyatt 1994) [45]:

$$U = U_c \times K \quad (1)$$

Where U_c = Combined standard uncertainties and K = coverage factor. Here we considered K=2 for normal distribution at 99% interval and Uc was calculated using eqn. 2 according to Taylor and Kuyatt [45].

$$U_c = \sqrt{\sum(Stdev_1{}^2 + Stdedv_2{}^2 + \cdots \ldots \ldots \ldots .. + Stdedv_n{}^2)} \quad (2)$$

So, U_c for MEKP = $\sqrt{\sum 0.29^2 + 0.34^2 + 0.2^2 + 0.014^2)}$ = 0.489

And U for MEKP = 0.489 * 2 = 0.98

Similarly, we calculated U_c for HMTD = $\sqrt{\sum 0.29^2 + 0.34^2 + 0.26^2 + 0.003^2)}$ = 0.517, and

And U for HMTD = 0.517 * 2 = 1.03

U_c for TATP = $\sqrt{\sum 0.29^2 + 0.34^2 + 0.33^2 + 0.041^2)}$ = 0.557, and

And U for TATP = 0.557 * 2 = 1.1

Conclusions

The current study demonstrates the ability to differentiate OPEs from background H_2O_2 using acid hydrolysis. The mechanism of differentiation of OPE signals from the ubiquitous H_2O_2 signals was confirmed by the mass spectral analysis of OPEs with/without H_2SO_4, corresponding to acid

484 condensation polymerization of MEKP and hydrolysis of HMTD and TATP. H_2SO_4 induced
485 degradation produced OPE derivatives with clear and selective FIA-CL signal, distinguishable from
486 the reduced FIA-CL signal intensity of H_2O_2. These structure specific signals afford the opportunity
487 of direct and rapid sampling, requiring minimal sample preparation prior to selective analysis,
488 and distinct from any possible source of confounding H_2O_2 seen in security screening
489 environments. The FIA-CL analytical working range had significantly improved LODs (TATP: 0.4
490 µM, HMTD: 0.43 µM, and MEKP: 0.4 µM). FIA-CL could find the balance between selective
491 analysis of OPEs and speed of analysis, with an arrangement that is feasibly deployable in security
492 environments with a need to detect trace OPE levels.

493 **Acknowledgements**

494 The authors gratefully acknowledge financial contribution of Defence Science Institute (DSI)
495 Australia (Grant ID: G12017SMahbubVU380) to Victoria University that enabled the authors to
496 conduct this investigation as part of the project. We also acknowledge contributions of Ms Jessica
497 San Diego and Mr Bryce Peter Cochrane, who worked as VU interns at various stages of the
498 project. This work was performed in part at the Melbourne Centre for Nanofabrication (MCN) in
499 the Victorian Node of the Australian National Fabrication Facility (ANFF).

500

501 **References**

502 [1] H. Schubert, A. Kuznetsov, Detection and disposal of improvised explosives, Springer Science &
503 Business Media2006.

504 [2] P. Mahbub, R. Wilson, P.N. Nesterenko, Ultra-fast continuous-flow photo degradation of organic
505 peroxide explosives for their efficient conversion into hydrogen peroxide and possible application,
506 Propellants Explos. Pyrotech. 41(4) (2016) 757-763.

[3] J.C. Oxley, J.L. Smith, K. Shinde, J. Moran, Determination of the vapor density of triacetone triperoxide (TATP) using a gas chromatography headspace technique, Propellants Explos. Pyrotech. 30(2) (2005) 127-130.

[4] R. Merrifield, T. Roberts, A comparison of the explosion hazards associated with the transport of explosives and industrial chemicals with explosive properties, IChemE Symposium, 1991, pp. 209-224.

[5] V. Krivitsky, B. Filanovsky, V. Naddaka, F. Patolsky, Direct and selective electrochemical vapor trace detection of organic peroxide explosives via surface decoration, Anal. Chem. 91(8) (2019) 5323-5330.

[6] S. Parajuli, W. Miao, Sensitive determination of triacetone triperoxide explosives using electrogenerated chemiluminescence, Anal. Chem. 85(16) (2013) 8008-8015.

[7] P. Mahbub, P. Zakaria, R. Guijt, M. Macka, G. Dicinoski, M. Breadmore, P.N. Nesterenko, Flow injection analysis of organic peroxide explosives using acid degradation and chemiluminescent detection of released hydrogen peroxide, Talanta 143 (2015) 191-197.

[8] R. Schulte-Ladbeck, A. Edelmann, G. Quintas, B. Lendl, U. Karst, Determination of peroxide-based explosives using liquid chromatography with on-line infrared detection, Anal. Chem. 78(23) (2006) 8150-8155.

[9] F. Rowell, J. Seviour, A.Y. Lim, C.G. Elumbaring-Salazar, J. Loke, J. Ma, Detection of nitro-organic and peroxide explosives in latent fingermarks by DART-and SALDI-TOF-mass spectrometry, Forensic Sci. Int. 221(1-3) (2012) 84-91.

[10] J. Kozole, L.A. Levine, J. Tomlinson-Phillips, J.R. Stairs, Gas phase ion chemistry of an ion mobility spectrometry based explosive trace detector elucidated by tandem mass spectrometry, Talanta 140 (2015) 10-19.

[11] Z. Can, A. Uzer, K. Turkekul, E. Ercag, R. Apak, Determination of triacetone triperoxide with a N, N-Dimethyl-p-phenylenediamine sensor on nafion using Fe3O4 magnetic nanoparticles, Analytical chemistry 87(19) (2015) 9589-9594.

[12] J.C. Oxley, J.L. Smith, L.J. Kirschenbaum, S. Marimganti, S. Vadlamannati, Detection of explosives in hair using ion mobility spectrometry, J. Forensic Sci. 53(3) (2008) 690-693.

[13] D. Martinak, A. Rudolph, Explosives detection using an ion mobility spectrometer for airport security, Proceedings IEEE 31st Annual 1997 International Carnahan Conference on Security Technology, IEEE, 1997, pp. 188-189.

[14] A.J. Marr, D.M. Groves, Ion mobility spectrometry of peroxide explosives TATP and HMTD, Int. J. Ion Mobil. Spectrom 6 (2003) 59-62.

[15] Z. Du, T. Sun, J. Zhao, D. Wang, Z. Zhang, W. Yu, Development of a plug-type IMS-MS instrument and its applications in resolving problems existing in in-situ detection of illicit drugs and explosives by IMS, Talanta 184 (2018) 65-72.

[16] M. Maziejuk, M. Szyposzyńska, A. Spławska, M. Wiśnik-Sawka, M. Ceremuga, Detection of Triacetone Triperoxide (TATP) and Hexamethylene Triperoxide Diamine (HMTD) from the Gas Phase with Differential Ion Mobility Spectrometry (DMS), Sensors 21(13) (2021) 4545.

544 [17] D.-D. JIANG, P. Li-Ying, Z. Qing-Hua, C. Chuang, L. Ji-Wei, W. Shuang, L. Hai-Yang, Quantitative
545 detection of hexamethylene triperoxide diamine in complex matrix by dopant-assisted photoionization
546 ion mobility spectrometry, Chinese J. Anal. Chem. 44(11) (2016) 1671-1678.

547 [18] M. Fitzgerald, D. Bilusich, Sulfuric, hydrochloric, and nitric acid-catalyzed triacetone triperoxide
548 (TATP) reaction mixtures: an aging study, J. Forensic Sci. 56(5) (2011) 1143-1149.

549 [19] A.C. van Duin, Y. Zeiri, F. Dubnikova, R. Kosloff, W.A. Goddard, Atomistic-scale simulations of the
550 initial chemical events in the thermal initiation of triacetonetriperoxide, J. Am. Chem. Soc. 127(31) (2005)
551 11053-11062.

552 [20] P.A. Fletcher, Kevin, N.; Calokerinos, A. C.; Forbes, Stuart; Worsfold, P. J., Analytical applications of
553 flow injection with chemiluminescence detection - a review, Luminescence 16 (2001) 1-23.

554 [21] R.S. Minhas, D.A. Rudd, H.Z. Al Hmoud, T.M. Guinan, K.P. Kirkbride, N.H. Voelcker, Rapid detection of
555 anabolic and narcotic doping agents in saliva and urine by means of nanostructured silicon SALDI mass
556 spectrometry, ACS Appl. Mater. Interfaces 12(28) (2020) 31195-31204.

557 [22] R. Burrows, J. Parr, Evaluating the goodness of instrument calibration for chromatography
558 procedures, LCGC Supplements 18(11) (2020) 35-38.

559 [23] D. Armitt, P. Zimmermann, S. Ellis-Steinborner, Gas chromatography/mass spectrometry analysis of
560 triacetone triperoxide (TATP) degradation products, Rapid Commun. Mass Spectrom. 22(7) (2008) 950-
561 958.

562 [24] Y.B. Tsaplev, Decomposition of cyclic acetone peroxides in acid media, Kinet. Catal. 53(5) (2012) 521-
563 524.

564 [25] W. Horwitz, L.R.Kamps., K. W. Boyer, Quality assurance in the analysis of foods and trace constituents,
565 J Assoc Off Anal Chem 63(6) (1980) 1344-54.

566 [26] N.A. Milas, A. Golubović, Studies in organic peroxides. XXV. Preparation, separation and identification
567 of peroxides derived from methyl ethyl ketone and hydrogen peroxide, J. Am. Chem. Soc. 81(21) (1959)
568 5824-5826.

569 [27] M.-H. Yuan, C.-M. Shu, A.A. Kossoy, Kinetics and hazards of thermal decomposition of methyl ethyl
570 ketone peroxide by DSC, Thermochim. Acta 430(1-2) (2005) 67-71.

571 [28] T.G. Burdo, W. R. Seitz, Mechanism of cobalt catalysis of luminol chemiluminescence, Analytical
572 Chemistry 47(9) (1975) 1639-1643.

573 [29] T. Krawczyk, Enhanced electrospray ionization mass spectrometric detection of hexamethylene
574 triperoxide diamine (HMTD) after oxidation to tetramethylene diperoxide diamine dialdehyde (TMDDD),
575 Rapid Commun. Mass Spectrom. 29(23) (2015) 2257-2262.

576 [30] J.C. Oxley, J.L. Smith, M. Porter, L. McLennan, K. Colizza, Y. Zeiri, R. Kosloff, F. Dubnikova, Synthesis
577 and degradation of hexamethylene triperoxide diamine (HMTD), Propellants Explos. Pyrotech. 41(2)
578 (2016) 334-350.

579 [31] H. Östmark, S. Wallin, H.G. Ang, Vapor pressure of explosives: a critical review, Propellants Explos.
580 Pyrotech. 37(1) (2012) 12-23.

581 [32] H. Jiang, G. Chu, H. Gong, Q. Qiao, Tin chloride catalysed oxidation of acetone with hydrogen peroxide
582 to tetrameric acetone peroxide, J. Chem. Res. 23(4) (1999) 288-289.

[33] R.I. Hiyoshi, J. Nakamura, T.B. Brill, Thermal decomposition of organic peroxides TATP and HMTD by t-jump/FTIR spectroscopy, Propellants Explos. Pyrotech. 32(2) (2007) 127-134.

[34] C. Black, T. D'Souza, J.C. Smith, N.G. Hearns, Identification of post-blast explosive residues using direct-analysis-in-real-time and mass spectrometry (DART-MS), Forensic Chem. 16 (2019) 100185.

[35] A. Arman, S.e. Sağlam, A.e. Üzer, R.a. Apak, Direct electrochemical determination of peroxide-type explosives using well-dispersed multi-walled carbon nanotubes/polyethyleneimine-modified glassy carbon electrodes, Anal. Chem. (2021).

[36] A. Üzer, S. Durmazel, E. Erçağ, R. Apak, Determination of hydrogen peroxide and triacetone triperoxide (TATP) with a silver nanoparticles—based turn-on colorimetric sensor, Sens. Actuators B 247 (2017) 98-107.

[37] L. Dunn, H.S.A. Al Obaidly, S.E. Khalil, Development and validation of fast liquid chromatography high-resolution mass spectrometric (LC-APCI-QToF-MS) methods for the analysis of hexamethylene triperoxide diamine (HMTD) and triacetone triperoxide (TATP), Forensic Chem. 10 (2018) 5-14.

[38] J.C. Mbah, S. Steward, N.O. Egiebor, Solid membrane electrode assembly for on board detection of peroxides based explosives, Sens. Actuators B 222 (2016) 693-697.

[39] S. Fan, J. Lai, P.L. Burn, P.E. Shaw, Solid-state fluorescence-based sensing of TATP via hydrogen peroxide detection, ACS Sens. 4(1) (2019) 134-142.

[40] N. Bagheri, A. Khataee, J. Hassanzadeh, B. Habibi, Visual detection of peroxide-based explosives using novel mimetic Ag nanoparticle/ZnMOF nanocomposite, J. Hazard. Mater. 360 (2018) 233-242.

[41] C. Costa, E.M. van Es, P. Sears, J. Bunch, V. Palitsin, K. Mosegaard, M.J. Bailey, Exploring rapid, sensitive and reliable detection of trace explosives using paper spray mass spectrometry (PS-MS), Propellants Explos. Pyrotech. 44(8) (2019) 1021-1027.

[42] J. Frazier, V. Benefield, M. Zhang, Practical investigation of direct analysis in real time mass spectrometry for fast screening of explosives, Forensic Chem. 18 (2020) 100233.

[43] B. Gökdere, A. Üzer, S. Durmazel, E. Erçağ, R. Apak, Titanium dioxide nanoparticles–based colorimetric sensors for determination of hydrogen peroxide and triacetone triperoxide (TATP), Talanta 202 (2019) 402-410.

[44] UNECE Classification of Organic Peroxides, Part 2 (2022), https://unece.org/DAM/trans/danger/publi/adr/adr2003/English/Part2_b.pdf, accessed 30 Dec 2022

[45] B.N. Taylor, C.E. Kuyatt, Guidelines for Evaluating and Expressing the Uncertainty of NIST Measurement Results, United States Department of Commerce Technology Administration, National Institute of Standards and Technology (NIST)Technical Note 1297, 1994 Edition, 1994, pp. 24.